



PAPER

Surface and near-surface dose measurements at beam entry and exit in a 1.5 T MR-Linac using optically stimulated luminescence dosimeters

RECEIVED
12 September 2019REVISED
3 December 2019ACCEPTED FOR PUBLICATION
20 December 2019PUBLISHED
12 February 2020Anthony Kim^{1,2,4,5} , Stephanie Lim-Reinders^{1,3}, Syed Bilal Ahmad¹ , Arjun Sahgal^{1,2} and Brian M Keller^{1,2}¹ Sunnybrook Health Sciences Centre/Odette Cancer Centre, 2075 Bayview Ave, Toronto, ON M4N 3M5, Canada² Faculty of Medicine, Department of Radiation Oncology, University of Toronto, 149 College Street, Suite 504, Toronto, Ontario M5T 1P5, Canada³ Faculty of Medicine, University of Toronto, Medical Sciences Building, 1 King's College Circle, Toronto, ON M5S 1A8, Canada⁴ Sunnybrook Health Sciences Centre, 2075 Bayview Avenue Toronto, ON M4N 3M5 Ontario, Canada⁵ Author to whom any correspondence should be addressed.E-mail: Anthony.Kim@sunnybrook.ca**Keywords:** MR-Linac, optically stimulated luminescence dosimeters, MRIgRT, surface dose, electron return effect, Monte Carlo treatment planning system**Abstract**

The objective of this study is to measure surface and near-surface dose at entry and exit surfaces in a 1.5 T MR-Linac (Elekta AB, Stockholm, Sweden) using optically stimulated luminescence dosimeters (OSLDs). OSLDs were expected to be useful for measuring surface dose in a strong magnetic field because they can be taped to undersides to measure exit dose, and their dose response have been shown to be reasonably insensitive to variations in beam angle, beam energy, and magnetic fields.

The surface and near-surface dose at the entry and exit of a 20 cm thick solid water phantom was measured with OSLDs for 5×5 , 10×10 , and 22×22 cm² field sizes. The solid water phantom was elevated off the couch top to produce an air gap of 3.7 cm so as to observe the electron return effect (ERE) near the beam exit surface. Measurement depths ranged from surface to 15 mm deep from entry and exit surfaces. The phantom dose distribution was also computed in the Monaco (Elekta AB, Stockholm, Sweden) Monte Carlo treatment planning system (TPS).

For the 5×5 , 10×10 , and 22×22 cm² field sizes the surface dose at depth 0 mm was extrapolated from OSLD measurements to be 10.9%, 12.0%, and 13.5%. The surface entry dose was found to be far less field size-dependent compared to a conventional linac, likely due to a lack of electronic contamination due to the strong magnetic field perpendicular to the beam. The ERE effect was observed in the measurements near the exit surface of the phantom, and was in close agreement with the TPS calculation.

Introduction

The MR-Linac is a promising new technology in radiation oncology. Worldwide, cancer centers have begun treating with clinical versions of a commercialized 1.5 T MR-Linac (Elekta AB, Stockholm, Sweden) with the goal of ever-increasing accuracy of radiotherapy plan delivery (Legendijk *et al* 2014, Raaijmakers *et al* 2017). Daily soft tissue visualization in the MR-Linac can potentially improve outcomes by enhancing dose conformity to deformable tumors, sparing organs-at-risk (OAR) and decreasing daily setup errors, providing an ideal platform to test the clinical efficacy of online adaptive radiation therapy (Lim-Reinders *et al* 2017).

One unique concern with the MR-Linac is the electron return effect (ERE), a phenomenon that is due to the ever-present magnetic field. The ERE is a consequence of electrons exiting tissue into air or low density organs, and then curling back due to the Lorentz force to deposit an elevated dose at the tissue interface (Raaijmakers *et al* 2008, Ahmad *et al* 2016a). This is particularly important for the skin where beams exit the body. Consequently, the potential for skin reactions poses a potentially limiting factor with MR-Linac treatments, particularly for some organs such as the breast (Kim *et al* 2017). As a result, it is important to quantify and characterize the surface

dose in an MR-Linac. Previous simulated studies have anticipated a dose peak at tissue-air interfaces at beam exit points based on Monte Carlo simulations (Ahmad *et al* 2016a, 2016b, 2017). However, there is limited reported data on the measurement of in-beam surface dose in an MR-Linac, with some work done with surface dose and interface effects measured by radiochromic film (Paudel *et al* 2016, Woodings *et al* 2018).

The reason for this is that surface dosimetry in an MR-Linac is quite challenging. In a conventional linac, surface dose can be measured with parallel plate ionization chambers with a high level of accuracy and confidence (Rawlinson *et al* 1992). In an MR-Linac, use of parallel plate chambers is complicated, particularly for exit dose. Many chambers and the cables attached to them contain metallic or ferromagnetic components rendering them unsafe for use in MRI. Furthermore, the air gap between the two plates introduces its own ERE, resulting in changes in dose response that is highly angularly dependent and requires large correction factors (Malkov and Rogers 2018). Radiochromic film is another detector that might be employed to measure surface dose in an MR-Linac, such as the work by Hackett and co-workers to measure out-of-field surface dose due to spiraling electrons generated from the primary beam hitting a medium (Hackett *et al* 2018). However, film has several drawbacks. Film calibration curves are dependent on manufacturing batch, location and orientation on a flatbed scanner, and post-irradiation time. Film is also sensitive to dust, smudges, imperfections, and inaccuracies at the cut edges. Finally, film has a highly non-linear dose response curve, meaning the percent accuracy greatly varies depending on the dose deposited. The uncertainties associated with film make it difficult to use as a dosimeter to determine surface dose.

We propose that optically stimulated luminescence dosimeters (OSLDs) are a possible solution to the problem of measuring surface dose in an MR-Linac. OSLDs are small, low profile, and can be made near-flush to the measurement surface. They are solid-state devices that are largely angularly independent and energy independent in the MV range (Jursinic 2007). They can be taped to surfaces, so measuring the exit dose in a phantom or patient at lateral or undercut angles is possible. They have also been demonstrated as MR-safe (Tchistiakova *et al* 2017). In many ways, OSLDs are an evolution of thermoluminescence dosimetry, which has also been successfully used to measure surface dose measurement such as in the extrapolation method of Kron and co-workers (Kron *et al* 1996); however, OSLDs have the advantages of simpler and faster read-out, multiple read-outs without dose erasure, and far less bulky annealing and measurement equipment. Overall, OSLDs are well-validated tools for dosimetry and have potential to be translatable as surface dosimeters in an MR-Linac.

The objective of this study is to use OSLDs in a 1.5 T MR-Linac to characterize the surface dose at entry and exit surfaces, which is currently under-reported in the literature. We started off by using OSLDs in a conventional linac to calibrate them as well as to determine the OSLD water equivalent thickness (WET), then employing them to measure surface and near-surface dose for various field sizes in the MR-Linac. We also simulated the phantom irradiations in a Monte Carlo-driven treatment planning system (TPS) to compare to the measurements.

Methods

Calibration of OSLDs to reduce error

To measure the surface and near-surface dose in an MR-Linac, we used nanoDot OSLDs (Landauer, Glenwood, USA). NanoDots have a small profile, measuring $10 \times 10 \times 2$ mm. They can be easily read out by the Landauer OSLD microStar reader by inserting them in the reader and turning a knob. Furthermore, each OSLD can be ‘optically annealed’ to zero the dose in an appropriate light irradiator and used again. NanoDots come with a factory-established calibration factor that is associated with a given manufacturing batch. These are then further screened to eliminate the nanoDots that are outside of the vendor’s tolerance band for accuracy. According to our own internal quality assurance program, the nanoDots are accurate to within a tolerance band of $\pm 3\%$. To improve upon the accuracy, the nanoDots were individually calibrated in-house. The OSLD dose reading, with the calibration factor, then provides a more accurate dose measurement than without the calibration factor.

To calibrate each OSLD, we irradiated them with a known dose in a conventional linac, a Versa HD (Elekta AB, Stockholm, Sweden) with a flattened 6 MV beam. The linac calibration was performed using a Farmer-style NE-2571 ionization chamber with a calibration factor traceable to the National Research Council of Canada. The procedures prescribed by the American Association of Physicists in Medicine Task Group 51 (Almond *et al* 1999) and its addendum (McEwen *et al* 2014) were followed. We placed four OSLDs in a polystyrene holder mounted on top of 10 cm of solid water (Gammex RMI, Middleton, WI) (figure 1). Then we placed a further 10 cm of solid water on top and set the dosimeter plane to 100 cm from the target (the isocentric plane). A 10×10 field was delivered, and with knowledge of the tissue phantom ratio (TPR) and the machine output (which was measured immediately prior to the experiment), the dose to the isocentric plane was calculated. The OSLDs were then read out in the Landauer microStar reader. The ratio of the known dose delivered and the OSLD read dose is the calibration factor for the given dosimeter. We calibrated 50 OSLDs in this way for this study.

In order to quantify the new accuracy band of the OSLDs with use of this new calibration factor, we zeroed the OSLDs and then repeated the experiment and irradiated the OSLD under the same conditions.

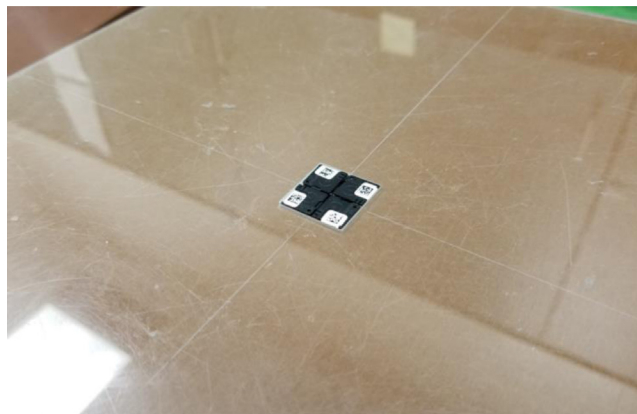


Figure 1. OSLDs embedded in a polystyrene holder (2 mm thick to match the OSLD thickness), enabling stacks of solid water to be placed on top.

Zeroing the OSLDs

OSLDs can be zeroed, i.e. the vast majority of the dose signal removed from the sensitive material, by exposing the $\text{Al}_2\text{O}_3\text{:C}$ material to a bright light over a period of several hours. The OSLD sensitive material was exposed by extracting the dosimeter disc cartridge. The OSLD was then placed on an x-ray light box powered by fluorescent light bulbs (figure 2). Prior to use, the light box surface was carefully cleaned with alcohol wipes to remove any dust. Once a collection of OSLDs were exposed in this way, one-half of an optical integrating sphere was placed over the OSLDs. The integrating sphere has a specular reflective coating on the interior, such that any light emitting from the x-ray light box bounces back off the coating, multiplying the light fluence on the OSLD sensitive material. Previous experiments demonstrated that exposure of these OSLDs to this environment erases nearly all of the dose signal such that after 8 h <0.1 cGy remains, which is negligible signal compared to the dose levels read out in this study.

There is a dose limit to how many times OSLDs can be irradiated and zeroed before changes in sensitivity become problematic. The vendor, Landauer, specifies this limit at a total dose of 15 Gy. Throughout this study, no OSLD that we used exceeded 7.5 Gy total dose.

Determination of WET with and without the OSLD casing

Previous reports have leveraged the Landauer nanoDot's construction by using it for measurement without the protective casing to obtain a near-surface dose measurement (Yusof 2015). As mentioned previously, the OSLD sensitive material may be extracted and even removed from the casing (figure 3). The exposed material has a putatively shallower WET than with the casing. The benefit to using two different configurations is the ability to measure at two different near-surface depths.

We have designated the two configurations as:

OSLD_c: with sensitive material within the casing.

OSLD_x: with the sensitive material extracted and removed from the casing.

To quantify the WET of the OSLD_c and OSLD_x configurations, the dose from surface to the depth-of-maximum-dose (d_{max}) was measured with the two different OSLD configurations as well as with an Attix parallel plate chamber. The Attix chamber was used to provide a 'ground truth' for surface-to-build-up-region dose, as a dose reading without any build-up on the Attix is considered to be close to the true surface dose (Rawlinson 1992, Reynolds and Higgins 2015). This experiment was done in an Elekta Versa HD conventional linac with a 6 MV flattened beam. Although it would have been ideal to do this WET experiment in the MR-Linac itself, we were unable to due to ferromagnetic components in the Attix chamber cable, as well as a lack of knowledge of the dose response of the Attix to the high magnetic field. Using varying thicknesses of solid water and adjustment of the couch height, a percent depth dose (PDD) curve with source-to-surface-distance (SSD) of 100 cm was built with depths from surface/near-surface to d_{max} . The depth of maximum dose and the normalization point of each of the PDD curves were taken to be $d_{\text{max}} = 15$ mm. This normalization point was justified because it was expected that the two different OSLD configurations would have WETs in the sub-mm range, and the dose variance of a 6 MV beam ± 1 mm from the true peak is negligibly small for the purposes of this WET experiment. PDD curves were measured for a 6 MV beam and 5×5 and 10×10 cm² field sizes, with two OSLDs for each measurement depth. The overlaying solid water was varied from no solid water at all for near surface dose, and also for 1, 2, 3, 5, and 15 mm.



Figure 2. Zeroing the OSLDs with an x-ray light box. The integrating sphere, when placed on top of the OSLDs, multiplies the light fluence incident on the dose-sensitive material.

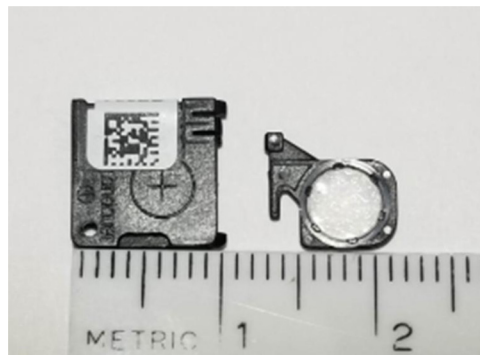


Figure 3. OSLD_c and OSLD_x configurations, i.e. with and without the protective casing.

By graphing the PDD curves for the Attix, OSLD_c, and OSLD_x dosimeters, the WET can be extracted by averaging the distance between the Attix chamber and OSLD curves (for both OSLD_c and OSLD_x).

Surface and near-surface dose measurement in the MR-Linac

Once the OSLDs were calibrated and the WET determined, they could be put to use in the MR-Linac for the dose measurement of surface-to-build-up-region at the entry and exit of a phantom.

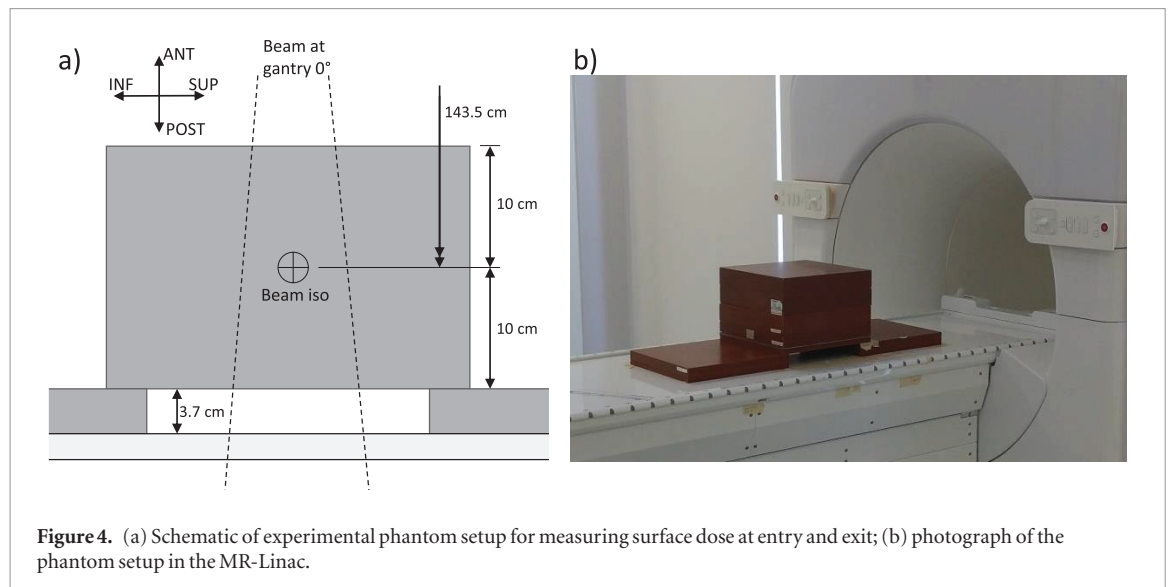
The MR-Linac is called Unity (Elekta AB, Stockholm, Sweden). The machine is a bore-type MRI nested within a gantry that carries a linac that rotates about the same axis as the MRI magnet. The beam irradiates through the MRI's cryostat between a gap in the main magnet's coils. The magnetic field is 1.5 T, so the beam irradiates the patient in the presence of a strong, transverse magnetic field.

The phantom was built of solid water slabs and constructed such that the entry and exit doses may be measured (see figure 4). It consists of 20 cm of solid water mounted on top of two smaller stacks of solid water 3.7 cm in height, with the smaller stacks spaced apart such that there is a substantial air gap between the bottom of the 20 cm stack and the table. The air gap is so placed such that exit dose measurements may be taken. With this setup, the source-to-surface distance (SSD) was 133.5 cm, and the surface was 10 cm above the MRI/radiation nominal isocentre.

Raaijmakers and co-workers demonstrated using a Monte Carlo study that the radius of exiting electron trajectories in a vacuum under influence of a 1.5 T magnetic field is 14.5 mm for a 6 MeV electron; for less energetic electrons, the radius is proportionally smaller (Raaijmakers 2005). This suggests that the 3.7 cm air gap between the solid water phantom and the table is sufficiently large enough that returning electrons will not be stopped by the table.

In taking entry and exit surface/build-up dose measurements with the OSLDs, the SSD to the entry surface was maintained, and the height above the table was maintained. For each depth of dose measurement, solid water plates were added or subtracted to embed the OSLD dosimeters at varying depths.

For the surface-to-build-up dose measurement, 5×5 , 10×10 , and 22×22 cm² field sizes were used. The gantry was set to 0° for all irradiations. The number of monitor units delivered was such that the doses given to



the OSLDs would be in approximately the 50–250 cGy range, which is within the reliably linear dose response range for the OSLDs.

For every depth of measurement and field size, two OSLD dose measurements were taken with the results averaged. As described later in the Results, the WET values for the OSLDs that were determined from depth dose measurements with the Attix ionization chamber were 0.16 mm and 0.64 mm for the OSLD_x and OSLD_c configurations.

For depth = 0.16 mm at entry

For the nearest-surface dose measurement at entry, OSLDs in the OSLD_x configuration were placed at the surface of the phantom (WET = 0.16 mm), with the dosimeter centre within a radius of 5 mm from the central axis (CAX). The CAX was localized by imaging a radio-opaque pointer using the MR-Linac's portal imager. The room lights were dimmed during and after irradiation, which is important as the sensitive volume in the OSLD_x configuration was exposed to the ambient light. The OSLDs in the 'exposed' configuration were exposed to the ambient light typically <1 min post-irradiation. Jursinic demonstrated that it takes 100 min in dim room light for the exposed sensitive volume to dissipate by 20%, so it was expected that exposing the OSLD_x post-irradiation for <1 min while inside an unlit MRI bore would result in negligible dissipation of the dose reading (Jursinic 2007).

For depth = 0.16 mm at exit

For the exit dose, we found that it was difficult to tape the sensitive disc in the OSLD_x configuration with intimate contact to the underside of the phantom. The device would not fully contact the underside of the surface since the lip of the device did not provide enough surface area to tape effectively, as it was important to not put tape over the dose-sensitive disc itself. Our solution was to take the 0.16 mm exit dose measurement with the OSLD_x on the anterior surface of the phantom and the gantry rotated to 180°, so that gravity would pull the sensitive disc in close contact with the phantom surface. We also took measurements with the OSLD_c configuration at gantry 180° so as to ‘stitch’ the gantry 0° exit data with the gantry 180° exit data at a matching point at depth 0.64 mm.

For depth = 0.64 mm

For the next most-shallowest measurement, an OSLD in the OSLD_c configuration was placed at the phantom surface (WET = 0.64 mm), again with the dosimeter centre within a radius of 5 mm. When taping OSLD_c to the underside of the phantom, care was taken to not place tape directly over the sensitive OSLD disc. We did not have the same issues taping OSLD_c to the underside of the phantom as with the OSLD_x configuration, as the nanoDot casing was substantial enough in surface area to firmly tape the device upside-down without it losing contact with the phantom surface.

For depths = 3, 5, 10, 15 mm

For all other sub-surface measurements at varying depths within the build-up region, the OSLDs were embedded within the same 2 mm thick polystyrene plate as shown in figure 1. As in the calibration experiment, this plate can hold $4 \times \text{OSLD}_c$ at the same time, and can be stacked square to the rest of the solid water phantom. Two OSLD_c 's were placed in two diagonal spaces, with two 'dummy' OSLD_c 's placed in the other two spaces so there would be

no air gaps. The centers of the OSLD sensitive volumes were thus within a 5 mm radius from the central axis. The center of the 2 mm thick polystyrene plate was taken as the dosimetric plane. The depths of measurement were varied by placing the plastic plate plus OSLD_c's at varying depths, placing different thicknesses of solid water over and under the dosimetric plane. For all of the field sizes and depths, it was expected that the area encompassing a 5 mm radius from the CAX would be homogeneous enough in dose so that if the centre of the OSLD sensitive disc was placed within this radius it would be representative of the CAX dose. Water tank commissioning data for the MR-Linac suggested highly uniform profiles at the depth of maximum dose within 5 mm from the CAX for field sizes of 5×5 , 10×10 , and 22×22 cm².

The OSLDs were read out between 30 min and 10 h after irradiation. Jursinic demonstrated that this post-irradiation window is a stable period of time to read out OSLDs (Jursinic 2007), which is also our experience using OSLDs for clinical purposes the past few years. The calibration factors for each individual OSLD were applied to the raw dose readings to produce a more accurate dose measurement result.

Monte Carlo TPS calculation of PDDs

The MR-Linac is driven by the Monaco TPS (v. 5.40.00, Elekta). The beam model simulates a 7 MV photon beam in the presence of a 1.5 T transverse magnetic field. In order to calculate magnetic field effects on the beam's interaction with media, Monaco employs a Monte Carlo dose calculation algorithm called GPUMCD, which has been validated by others in various media (Ahmad *et al* 2016a, 2016b).

It is instructive to compare TPS calculations with our OSLD measurements, hence we calculated the PDDs in a simulated phantom setup identical to shown in figure 4 in Monaco. For the calculation we used a 1 mm dose grid and 0.5% statistical uncertainty. The phantom in the TPS was a virtual phantom with electron density over-ridden to 1 g cc⁻¹.

Results

Calibration of OSLDs to reduce error

Each of the 50 OSLDs in our stock were irradiated with a known dose and then read out. The read dose had a standard deviation of 3.0% compared to the known dose, when solely using the factory calibration. This is in line with results from our quality assurance program for the OSLD reader, which also historically has been within approximately a $\pm 3\%$ band.

After the first irradiation, calibration factors were calculated by dividing the known dose with the read dose for each OSLD. Each OSLD was zeroed using the light annealing method previously described and then they were re-irradiated using the same procedure in a conventional linac. By applying the calibration factors, the read dose was now within $\pm 1.5\%$ standard deviation of the known dose, an improvement over the $\pm 3.0\%$ it would be without using individual calibration factors.

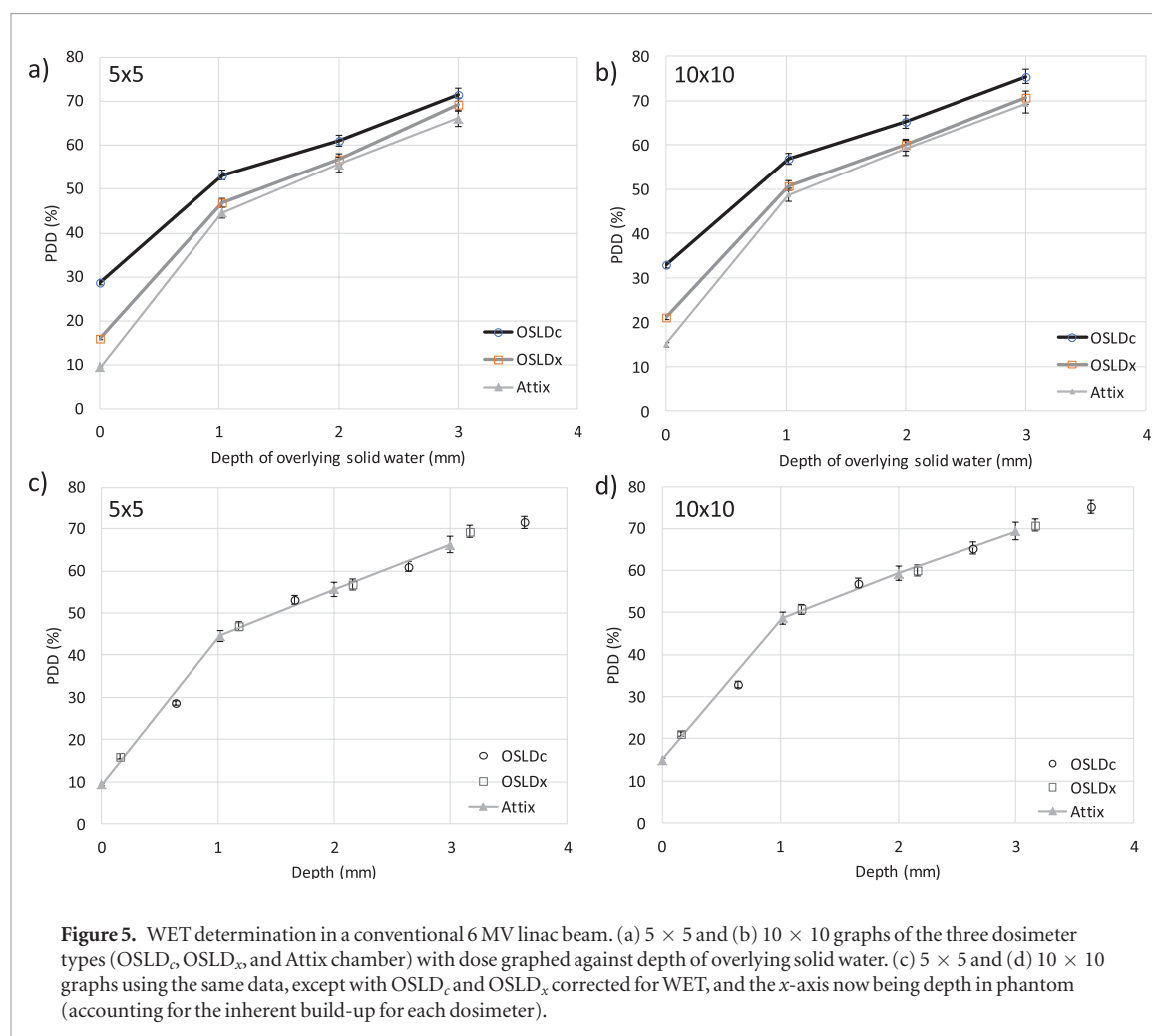
Determination of WET with and without the protective casing

In order to determine WET of OSLD_c and OSLD_x configurations, measurements in the surface and build-up regions using both these configurations were compared to an Attix chamber, which has been shown to require no correction factor when compared to extrapolation chamber measurements (Reynolds and Higgins 2015).

Figures 5(a) and (b) shows data for OSLD_c, OSLD_x, and Attix for 5×5 and 10×10 cm² field sizes. It was expected that the WET of both OSLD_c and OSLD_x configurations would be sub-mm, so it was considered reasonable to use $d_{\max} = 15$ mm as a static normalization point, regardless of the actual WET of the dosimeter. The WET for OSLD_c and OSLD_x was determined by printing out the graphs to a large scale and, with a ruler, measuring the distances between the OSLD_c and Attix curves, and the OSLD_x and Attix curves at 0, 1, and 2 mm of overlying solid water material. These distances were averaged for both field sizes. The result was a WET of 0.64 mm for OSLD_c and 0.16 mm for OSLD_x. As a comparison, another published Monte Carlo study measured WETs of 0.8 mm and 0.3 mm for the OSLD_c and OSLD_x configurations (Zhuang and Olch 2014), reasonably close to our results using direct measurements with the Attix chamber.

Figures 5(c) and (d) show the same 5×5 and 10×10 cm² data except correcting for the WET for OSLD_c and OSLD_x. The data are plotted against depth in phantom, which amalgamates the inherent build-up for each dosimeter as well as overlying phantom material. The OSLD data points now track closely to the Attix graph, demonstrating a reasonable estimation of the WETs.

For all graphs in figure 5, the error bar lengths were calculated from the standard deviations of the ratio distribution that results from computing the PDD, i.e. the dose at a depth divided by the dose at d_{\max} , all multiplied by 100%. In order to compute the ratio distribution standard deviations, the error standard deviations of each of the detectors were used. For the OSLDs, the error standard deviations for the dose measurements were $\pm 1.5\%$. For the Attix chamber, we used an error standard deviation of 2.1%, from the uncertainty estimated by the work of Reynolds and Higgins (Reynolds and Higgins 2015)



Extrapolating between the two OSLD points nearest the surface (i.e. the OSLD_c and OSLD_x data points), an estimation of the surface dose can be calculated and compared to the Attix chamber. For 5×5 cm² field size, the OSLD surface dose was 11.2% versus 9.4% for the Attix (1.8% difference); for the 10×10 cm², the OSLD method yielded a surface dose of 16.7%, against the Attix surface dose of 14.9% (again, 1.8% difference). This demonstrates that a two-point extrapolation method using the OSLD data can yield a reasonable estimate of the true surface dose at depth = 0 mm.

Surface and near-surface dose measurement in the MR-Linac

Figures 6(a), (c) and (e) shows the dose calculation of the axial dose distributions for the solid water phantom, for the 5×5 , 10×10 , and 22×22 cm² field sizes. Note the dose enhancement near the exit of the beam showing the ERE. Figures 6(b), (d) and (e) shows the Monaco dose calculation against the OSLD data, and shows good agreement viewed at a macroscopic level. Note that both measurements and TPS calculation shows the ERE with a ramping up of dose near the exit surface.

Figure 7 displays magnified views of the data at entry and exit. At entry and exit, all data points track closely to the TPS prediction.

Table 1 shows the figure 7 data with percent differences between TPS and measurement calculated for $d = 0.16$ to 15 mm. At entry, the percent difference ranges between -3.8% to 3.9% over all field sizes, omitting the one outlier at 3 mm depth for the 10×10 field size (-8.9%). At exit, the range is between -1.0% to 3.4% . Considering AAPM TG-53 recommendation of surface/near-surface dose to have $\pm 20\%$ agreement between TPS and measurement (Fraass *et al* 1998), these results are reasonable.

The surface dose data (i.e. $d = 0$ mm) can be estimated by extrapolating between the OSLD_x and the OSLD_c data points with no overlying solid water on top (as in the WET determination section). It is also fairly instructive to compare our results to another researcher's work—here we selected Oborn and co-workers' research on surface dose in a magnetic field as calculated by a Monte Carlo algorithm in a magnetic field (Oborn *et al* 2010). Oborn's work has an identical phantom to that used in our work, with the exception that the beam was a 6 MV beam and the SSD was 100 cm (for the MR-Linac it is 7 MV and SSD = 133.5 cm). This difference in SSD can be largely corrected for using a Mayneord factor.

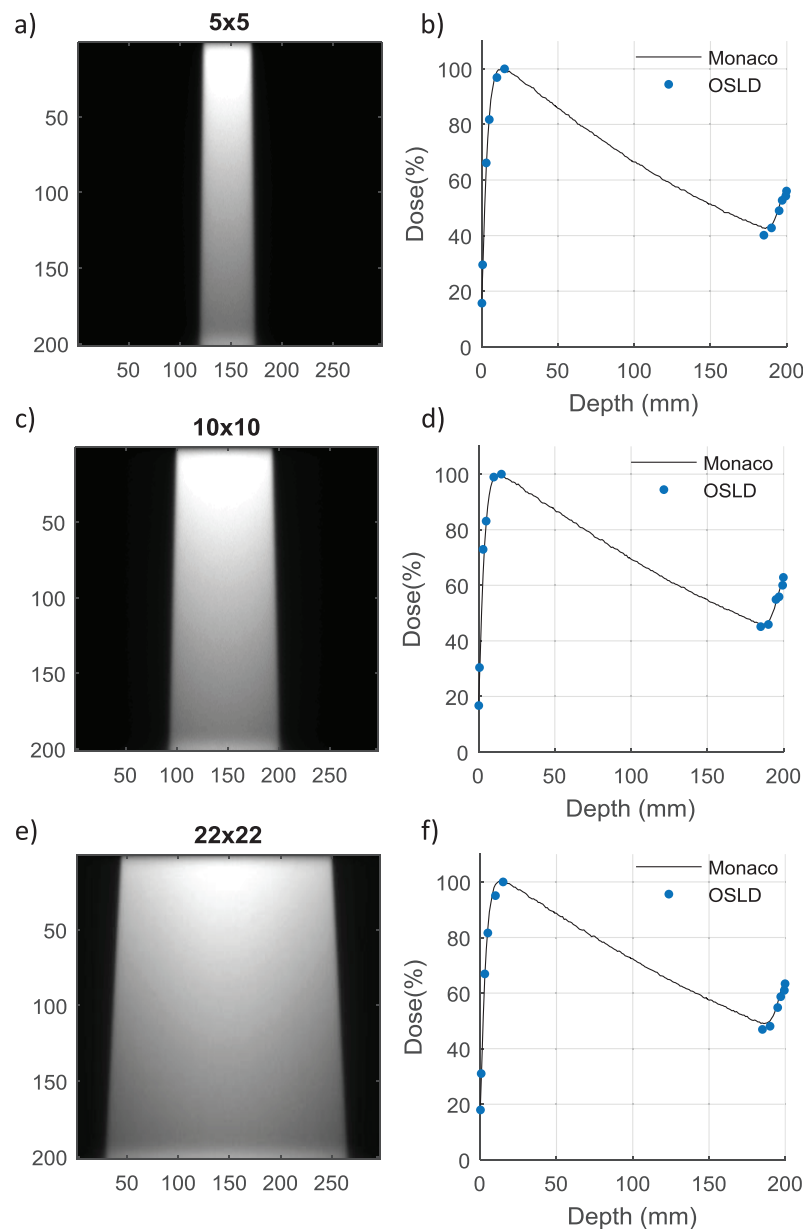


Figure 6. (a), (c) and (e) Axial dose distributions calculated in Monaco for 5×5 , 10×10 , 22×22 , note the enhanced dose at the exit; (b), (d) and (f) corresponding PDDs with the Monaco calculation overlaid with the OSLD measurements at entry and exit. Error bars are added in figure 7, where the entry and exit data are magnified.

Table 2 shows our OSLD data extrapolated to $d = 0$ mm, as well to $70 \mu\text{m}$ to compare to the work of Oborn ($70 \mu\text{m}$ is representative of the active skin layer, ICRP 1991). At $d = 0$ mm, there is a striking lack of field size-dependence at entry compared to the variation one would normally see in a conventional (i.e. no magnetic field) linac. Also, the comparison between our data at $d = 70 \mu\text{m}$ and the data of Oborn *et al* has very close agreement (within 1.28% for entry and 1.43% for exit).

Discussion

There are two major benefits of using a solid state detector such as an OSLD to characterize an MR-Linac beam's exit surface dose: the ability to tape it to angled or upside-down surfaces, and the thin construction of the sensitive volume. Measuring exit dose was as simple as taping an OSLD to the underside of the solid water phantom (although we ran into difficulties taping the OSLD_x configuration upside-down, but this might be simply solved in future with a better adhesion technique). A parallel plate ionization chamber is not an ideal surface dosimeter in an MR-Linac due to the difficulties of using air chamber dosimeters in a magnetic field (O'Brien and Sawakuchi 2017). Film may also be used in the simple way as the OSLDs in this study, with the same benefits of being tape-able to surfaces and thin construction; however, we did not use it in this study as film does

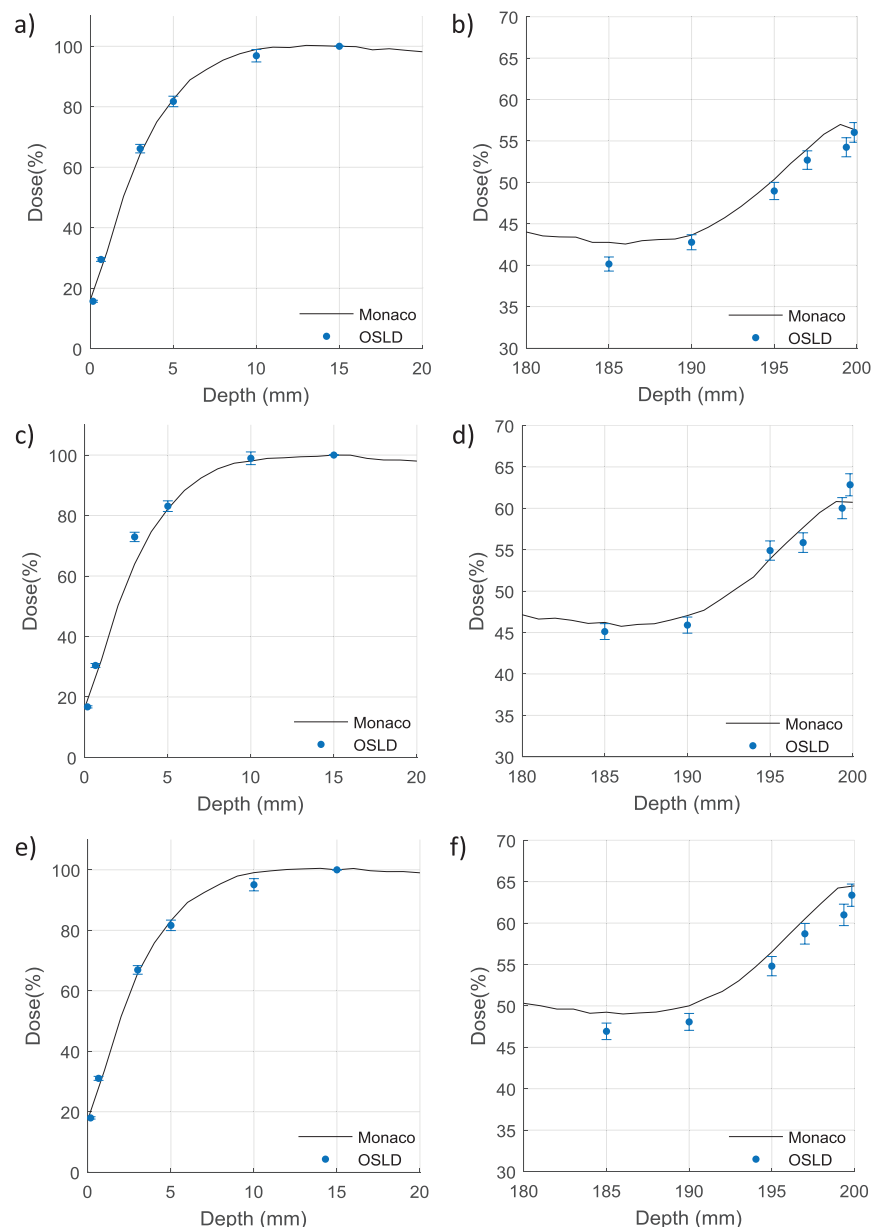


Figure 7. Magnified PDDs with Monaco calculation overlaid with the OSLD measurements. (a), (c) and (e) Entry PDDs for 5×5 , 10×10 , and 22×22 field sizes; (b), (d) and (f) Exit PDDs for the same field sizes. Error bar lengths are the error standard deviation of the ratio distribution when OSLDs are used to compute PDDs. Note there are no error bars at depth = 15 mm as this is the normalization point.

not have a linear response, and there are difficulties with ensuring accurate absolute dose determination because it relies so much on the state of the film scanner, film batch, cleanliness, cut edges, and where on the response curve the dose is read off.

There are other justifying reasons for using OSLDs for surface dose. OSLDs are appropriate for measurement of the ERE, as the material has a response curve that is flat with electron dose and the 7 MV energy range (Jursinic 2007). Also, OSLDs are relatively energy-independent in MV beams >1 MeV (Scarboro 2012), so beam quality differences whilst penetrating a water-like phantom are not expected to produce dose response problems for our study.

One detriment to using OSLDs for physics measurements in general is that it is not possible to immerse them in water without drastically losing dose accuracy. We tested immersing radiation-exposed OSLDs in water. After immersion and air-drying, OSLDs have a drop in read dose between -3.6% to -10.0% . The dose is always read out lower after water immersion, as if dose is ‘washed away’, or perhaps trapped electrons are perturbed by contact with water. This unpredictable error makes water as a phantom medium unusable with OSLDs, hence why we chose solid water as the phantom medium in this study.

Table 1. OSLD measurement versus TPS data at the various measurement depths for the three field sizes. Here, d is the distance to the nearest surface, whether entry or exit. Both measurement and TPS are normalized to the dose 15 mm from the beam entry surface for the given field size.

FS	d (mm)	ENTRY			EXIT		
		OSLD	TPS	% diff	OSLD	TPS	% diff
5×5	0.16	15.7	18.7	3.0	56.0	56.4	0.4
	0.64	29.5	26.3	−3.2	54.2	56.6	2.4
	3	66.2	64.4	−1.8	52.7	54.0	1.3
	5	81.8	82.5	0.7	49.0	50.6	1.6
	10	96.9	99.0	2.1	42.8	43.7	0.9
	15	100	100	n/a	40.1	42.8	2.7
10×10	0.16	16.7	19.0	2.3	62.8	60.7	−2.1
	0.64	30.4	26.6	−3.8	60.0	60.8	0.8
	3	72.9	64.0	−8.9	55.9	57.7	1.8
	5	83.1	82.2	−0.9	54.9	53.9	−1.0
	10	98.9	98.0	−0.9	45.9	47.0	1.1
	15	100	100	n/a	45.1	46.2	1.1
22×22	0.16	18.0	20.0	2.0	63.4	64.5	1.1
	0.64	31.0	27.8	−3.2	61.0	64.4	3.4
	3	66.9	65.9	−1.0	58.7	60.5	1.8
	5	81.6	83.2	1.6	54.8	56.5	1.7
	10	95.1	99.0	3.9	48.1	50.0	1.9
	15	100	100	n/a	46.9	49.2	2.3

Table 2. OSLD data extrapolated to the surface. Data also extrapolated to 70 μm to compare against Oborn *et al* Monte Carlo study on surface dose. Here, d denotes the distance to the nearest surface (whether at entry or exit).

	Field size	OSLD _c	OSLD _x	Extrap. OSLD to	Interp. OSLD to	Oborn <i>et al</i> ^a	%diff w/Oborn
		$d = 0.64$ mm	$d = 0.16$ mm	$d = 0$ mm	$d = 70$ μm	$d = 70$ μm	$d = 70$ μm
ENTRY	5×5	29.5	15.7	10.9	13.0	13.8	−0.8
	10×10	30.4	16.7	12.0	14.0	14.7	−0.6
	22×22	31.0	18.0	13.5	15.4	16.7	−1.3
EXIT	5×5	54.2	56.0	56.6	56.4	55.1	1.3
	10×10	60.0	62.8	63.8	63.4	62.0	1.4
	22×22	61.0	63.4	64.2	63.8	64.9	−1.0

Also, Oborn *et al* data shown here is for 5×5 , 10×10 , and 20×20 field sizes (22×22 was not done for that study).

^a Oborn *et al* data needed to be corrected from SSD = 100 cm to SSD = 133.5 cm for the Elekta MRI-Linac.

One of the weaknesses of this study is that there are sub-mm air gaps in the construction of the OSLD. For the OSLD_x configuration, there is an air gap of 0.25 mm between the sensitive disc and the solid water surface, as the disc itself is slightly raised up by the cartridge it is embedded in; for the OSLD_c configuration, there are sub-mm air gaps above and below the sensitive disc within the casing. These air gaps may alter the dose response due to the presence of the 1.5 T magnetic field. There is no obvious way of getting around this, as we have determined that using liquid (and probably gel) to close off air gaps will unpredictably decrease the dose reading. It turns out that the air gap effect on dose measurement is likely very minimal. OSLDs have been tested in magnetic fields from 0 to 1 T at depth 10 cm with only a −1.3% decrease in dose response per T (Spindeldreier *et al* 2017). Other work with TLDs, OSLDs, and radiochromic film have been done where the dosimeters were irradiated in an MR-Linac with and without a 1.5 T magnetic field (the magnet was ramped down at one point, giving opportunity to irradiate at 0 T)—these results also showed a very small dose response due to the magnetic field (−0.4%) (Wen *et al* 2016). If the magnetic field affects the OSLD dose response, and this effect is approximately the same at all depths, then normalizing the PDD to 15 mm may at least partially cancel out any magnetic field effects.

It is an inherent assumption in this work that the WETs measured in the Versa HD 6 MV beam are equivalent to the MR-Linac's 7 MV beam. It is necessary to make this assumption as it was not possible to do the WET test with the Attix chamber, as there is a lack of dose certainty in the MR-Linac due to uncharacterized ERE within the chamber itself. Moreover, parts of the Attix cable are ferromagnetic. We believe that the WET equivalency

assumption is reasonable as the quality of the two beams is very similar, which is indeed the case: the TPR depth 10 cm for the Versa HD 6 MV beam is 0.788 and for the MR-Linac it is 0.793 (0.6% difference).

The comparison with Oborn *et al* in table 2 supports our argument that OSLDs are a reasonable dosimeter to use for surface dosimetry. Our results match to within 1.3% to results from the Oborn study at 70 μm depth at entry. The exit surface dose results were slightly more widely varying (within 1.5%); however, it may be because the attenuation through 20 cm of phantom would be different for the Varian 6 MV beam in the Oborn study versus the 7 MV MR-Linac beam in our study.

There is one other study with published entry surface dose measurements in a 1.5 T MR-Linac which diverge from our results (Woodings *et al* 2018). In the Woodings study, surface dose is measured using radiochromic film coronally placed in a solid water phantom, offset by a few mm so that no primary ray is perfectly parallel to the film. A 90° beam irradiated the film such that the film essentially captured a slightly-off-axis PDD. Woodings reports entry surface doses for 5×5 , 10×10 , and 20×20 cm² field sizes as 34.6%, 35.8%, and 38.0% as read out from the film. These are quite different from our surface dose results for 5×5 , 10×10 , and 22×22 cm² field sizes as shown in table 2 (10.9%, 12.0%, 13.5%). We can only surmise that perhaps there was additional build-up of ~1 mm of film jutting out of the phantom that caused the elevated surface dose in the Woodings study, or perhaps there were cut-edge effects on the film near the phantom surface that affected the result. Our work is novel as we have presented surface dose at both entry and exit, and as the data are divergent from Woodings *et al* there is evidently further need for us and other researchers to investigate this matter.

Our results show a reduced field size dependence on surface dose compared to a conventional linac. From 5×5 to 22×22 cm², the surface dose at $d = 0$ mm varies by only $\Delta 2.5\%$. A recently commissioned Elekta Versa HD 6 MV flattening filter free (FFF) beam in our clinic (with no magnetic field) had measurements of surface dose ranging from 11.4%–23.8% ($\Delta 12.4\%$) for field sizes ranging from 5×5 to 20×20 cm². This reduced field size dependence may be explained by the lack of contaminant electrons in an MR-Linac, since these get swept away by the strong 1.5 T magnetic field. A large proportion of the surface dose in a conventional linac is due to contaminant electrons, which are known to be largely field size dependent. For an MR-Linac, the absence of these contaminant electrons might explain the dramatically reduced field size dependence on surface dose shown in this work.

Conclusion

We present the first measurements of surface and near-surface dose at both entry and exit in a 1.5 T MR-Linac using OSLDs. Surface entry dose is far less field size-dependent compared to a conventional linac, likely due to a lack of electronic contamination in a strong magnetic field. The ERE was shown in measurements near the exit surface of the phantom as a dose ramp-up. OSLDs are very useful as surface dosimeters. Follow up work will consist of implementing OSLD dosimetry for *in vivo* patient treatment dose verification.

ORCID iDs

Anthony Kim  <https://orcid.org/0000-0003-2609-6912>

Syed Bilal Ahmad  <https://orcid.org/0000-0003-0509-7537>

References

- Ahmad S B, Paudel M R, Sarfehnia A, Kim A, Pang G, Ruschin M, Sahgal A and Keller B M 2017 The dosimetric impact of gadolinium-based contrast media in GBM brain patient plans for a MRI-Linac *Phys. Med. Biol.* **62** N362–74
- Ahmad S B, Sarfehnia A, Kim A, Wronski M, Sahgal A and Keller B M 2016a Backscatter dose effects for high atomic number materials being irradiated in the presence of a magnetic field: a Monte Carlo study for the MRI Linac *Med. Phys.* **43** 4665
- Ahmad S B, Sarfehnia A, Paudel M R, Kim A, Hissoiny S, Sahgal A and Keller B 2016b Evaluation of a commercial MRI Linac based Monte Carlo dose calculation algorithm with GEANT4 *Med. Phys.* **43** 894–907
- Almond P R, Biggs P J, Coursey B M, Hanson W F, Huq M S, Nath R and Rogers D W 1999 AAPM's TG-51 protocol for clinical reference dosimetry of high-energy photon and electron beams *Med. Phys.* **26** 1847–70
- Fraass B, Doppke K, Hunt M, Kutcher G, Starkschall G, Stern R and Van Dyke J 1998 American Association of Physicists in Medicine Radiation Therapy Committee Task Group 53: quality assurance for clinical radiotherapy treatment planning *Med. Phys.* **25** 1773–829
- Hackett S L, van Asselen B, Wolthaus J W H, Bluemink J J, Ishakoglu K, Kok J, Lagendijk J J W and Raaymakers B W 2018 Spiraling contaminant electrons increase doses to surfaces outside the photon beam of an MRI-Linac with a perpendicular magnetic field *Phys. Med. Biol.* **63** 095001
- International Commission on Radiological Protection 1991 ICRP Publication 60, 1990 Recommendations of the International Commission on Radiological Protection *Ann. ICRP* **21** 1–3
- Jursinic P A 2007 Characterization of optically stimulated luminescent dosimeters, OSLDs, for clinical dosimetric measurements *Med. Phys.* **34** 4594–604
- Kim A, Lim-Reinders S, McCann C, Ahmad S B, Sahgal A, Lee J and Keller B M 2017 Magnetic field dose effects on different radiation beam geometries for hypofractionated partial breast irradiation *J. Appl. Clin. Med. Phys.* **18** 62–70

- Kron T, Butson M, Hunt F and Denham J 1996 TLD extrapolation for skin dose determination *in vivo* *Radiother. Oncol.* **41** 119–23
- Lagendijk J J, Raaymakers B W and van Vulpen M 2014 The magnetic resonance imaging-linac system *Semin. Radiat. Oncol.* **24** 207–9
- Lim-Reinders S, Keller B M, Al-Ward S, Sahgal A and Kim A 2017 Online adaptive radiation therapy *Int. J. Radiat. Oncol. Biol. Phys.* **99** 994–1003
- Malkov V N and Rogers D W O 2018 Monte Carlo study of ionization chamber magnetic field correction factors as a function of angle and beam quality *Med. Phys.* **45** 908–25
- McEwen M, DeWerd L, Ibbott G, Followill D, Rogers D W, Seltzer S and Seuntjens J 2014 Addendum to the AAPM's TG-51 protocol for clinical reference dosimetry of high-energy photon beams *Med. Phys.* **41** 041501
- O'Brien D J and Sawakuchi G O 2017 Monte Carlo study of the chamber-phantom air gap effect in a magnetic field *Med. Phys.* **44** 3830–8
- Oborn B M, Metcalfe P E, Butson M J and Rosenfeld A B 2010 Monte Carlo characterization of skin doses in 6 MV transverse field MR-Linac systems: effect of field size, surface orientation, magnetic field strength, and exit bolus *Med. Phys.* **37** 5208–17
- Paudel M R, Kim A, Sarfehnia A, Ahmad S B, Beachey D J, Sahgal A and Keller B M 2016 Experimental evaluation of a GPU-based Monte Carlo dose calculation algorithm in the Monaco treatment planning system *J. Appl. Clin. Med. Phys.* **17** 230–41
- Raaijmakers A J, Raaymakers B W and Lagendijk J J 2005 Integrating a MRI scanner with a 6 MV radiotherapy accelerator: dose increase at tissue-air interfaces in a lateral magnetic field due to returning electrons *Phys. Med. Biol.* **50** 1363–76
- Raaijmakers A J, Raaymakers B W and Lagendijk J J 2008 Magnetic-field-induced dose effects in MR-guided radiotherapy systems: dependence on the magnetic field strength *Phys. Med. Biol.* **53** 909–23
- Raaymakers B W et al 2017 First patients treated with a 15 T MR-Linac: clinical proof of concept of a high-precision, high-field MRI guided radiotherapy treatment *Phys. Med. Biol.* **62** L41–50
- Rawlinson J A, Arlen D and Newcombe D 1992 Design of parallel plate ion chambers for buildup measurements in megavoltage photon beams *Med. Phys.* **19** 641–8
- Reynolds T A and Higgins P 2015 Surface dose measurements with commonly used detectors: a consistent thickness correction method *J. Appl. Clin. Med. Phys.* **16** 358–66
- Scarboro S B, Followill D S, Kerns J R, White R A and Kry S F 2012 Energy response of optically stimulated luminescent dosimeters for non-reference measurement locations in a 6 MV photon beam *Phys. Med. Biol.* **57** 2505–15
- Spindeldreier C K, Schrenk O, Ahmed M F, Shrestha N, Karger C P, Greilich S, Pfaffenberger A and Yukihiro E G 2017 Feasibility of dosimetry with optically stimulated luminescence detectors in magnetic fields *Radiat. Meas.* **106** 346–51
- Tchistiakova E, Kim A, Song W Y and Pang G 2017 MR-safe personal radiation dosimeters *J. Appl. Clin. Med. Phys.* **18** 180–4
- Wen Z, Wang J, Jiang W, O'Brien D, Sawakuchi G and Ibbott G 2016 SU-G-BRB-08: Investigation on the magnetic field effect on TLDs, OSLDs, and gafchromic films using an MR-Linac *Med. Phys.* **43** 3632
- Woodings S J et al 2018 Beam characterisation of the 15 T MR-Linac *Phys. Med. Biol.* **63** 085015
- Yusof F H, Ung N M, Wong J H, Jong W L, Ath V, Phua V C, Heng S P and Ng K H 2015 On the use of optically stimulated luminescent dosimeter for surface dose measurement during radiotherapy *PLoS One* **10** e0128544
- Zhuang A H and Olch A J 2014 Validation of OSLD and a treatment planning system for surface dose determination in IMRT treatments *Med. Phys.* **41** 081720